Upper and lower plane bed revisited

K. Ohata[1], N. Hajime[1], and N. Izumi[2]

[1] Division of Earth and Planetary Sciences, Graduate School of Science, Kyoto University,

Kyoto, Japan

[2] Division of Field Engineering for the Environment, Faculty of Engineering, Hokkaido

University, Sapporo, Japan

Corresponding author: Koji Ohata (ohata.koji.24z@st.kyoto-u.ac.jp)

Key Points:

- Compiled experimental and observational data suggest a new definition of plane beds

- Previous definitions of upper and lower plane beds do not explain the dataset well

- The lower and upper plane beds are redefined as flat bedforms that appear when

  suspended load is inactive and active, respectively

Abstract

This study proposes a new definition of plane bed regimes. The upper plane bed is defined as a flat bedform that appears under conditions of active suspended load, whereas the lower plane bed forms when sediment particles are moved only by bed-load. Previous studies have recognized that two types of plane bed could be distinguished by shear stress, particle size, or flow regime. However, the compilation of a large amount of existing open-channel flow data indicates that the plane bed regimes cannot be differentiated by existing definitions. Newly produced phase diagrams indicate that plane bed data plot in two separate regions, and the gap between the two regions corresponds to the threshold condition of suspension. Further investigation is needed to understand the physical mechanisms generating lower plane beds and characterizations of parallel laminae from lower and upper plane beds.

Plain Language Summary

Bedforms are topographic features that appear at fluid–solid interfaces, such as river beds. Several types of bedform have been found, and "plane bed" is a type of bedform commonly observed in rivers. Previous studies have recognized that there are two types of plane beds and they could be distinguished by flow properties or bed particle size. However, this study finds that previous definitions of plane beds are inconsistent with existing river observation and experimental data. Therefore, we propose a new definition for plane beds. This study establishes that plane beds can be formed with a wider range of flow properties and bed particle sizes than previously considered.

40

41

1 Introduction

43 Bedforms and sediment transport have attracted great interest of sedimentologists and engineers,

44 as well as geomorphologists. Although the formation conditions of bedforms have been

45 examined by theoretical methods, such as linear stability analysis (e.g., Colombini & Stocchino,

46 2008), predicting the flow conditions of bedform phases remains challenging owing to the

47 complexity of relationships between flows and bedforms. Therefore, numerous laboratory

48 experiments (e.g., Gilbert, 1914; Guy et al., 1966; Taylor, 1971) and field observations (e.g.,

49 Colby & Hembree, 1955; Culbertson et al., 1972) have been conducted to obtain empirical

50 relationships between flows and bedforms. The compilation of large data sets, including

51 experiments and field observations, facilitates the understanding of the formation conditions of

52 bedforms in response to flow behavior in alluvial rivers using bedform phase diagrams.

53 Bedforms are vital for river management and reconstruction of paleo-flow conditions (Best,

54 2005). Thus, bedform phase diagrams have been proposed based on laboratory and field

55 observations (e.g., van den Berg & van Gelder, 1993). Recently, Ohata et al. (2017) proposed

56 bedform phase diagrams in three-dimensional parametric space, and their diagrams successfully

57 reconstructed paleo-flow conditions from sedimentary structures.

58   The plane bed is a representative type of bedform that is commonly observed on alluvial

59 river beds (e.g., Hauer et al., 2019), beach surfaces (Vaucher et al., 2018), and can be recorded as

60 parallel lamination in sandstone beds formed in various environments such as rivers (e.g.,

61 Mazumder & Van Kranendonk, 2013; Umazano et al., 2012) and submarine fans (e.g.,

62 Eggenhuisen et al., 2011; Jobe et al., 2012). In submarine environment, it is known that parallel

63 lamination commonly occurs in turbidites as T_b or T_d divisions (Bouma, 1962).

64   The plane bed phase is characterized by nearly flat topography and was initially referred

65 to as "the smooth phase of bedforms" (Gilbert, 1914; Owens, 1908). Later, Simons et al. (1961)

66 used the term "plane" to avoid confusion with the hydraulically smooth phase of flows. Owens

67 (1908) and Strahan et al. (1908) observed that the bedform phase changes from ripples to

68 antidunes with increasing flow discharge, and the smooth phase of bedform (i.e., plane bed)

69 develops in the intermediate condition between ripples and antidunes. In addition, Simons et al.

70 (1961) recognized that the plane bed phase also appears under the condition when bed shear

71 stress is lower than that forming ripples or dunes. Thus, two conditions of plane bed formation

72 have been recognized.

73   However, researchers have had differing opinions on the definition and formation

74 conditions of the two types of plane bed. The two types of plane bed have been classified

75 depending on (1) criticality of sediment motion (Simons et al., 1961; Simons & Richardson,

76 1962), (2) criticality of Froude number (Dey, 2014; Venditti, 2013), and (3) size of bed material

77 and flow intensity (Allen, 1968; Southard, 1971). Simons et al. (1961) recognized two conditions

78 of plane bed in their flume experiments—plane beds with and without sediment motion. Simons

79 et al. (1961) and Simons & Richardson (1962) also classified alluvial flows based on bedforms

80 into three regimes—a lower flow regime (plane beds without sediment movement, ripples, dunes

81 with ripples superposed, dunes), a transition zone (washed-out dunes), and an upper flow regime

82 (plane beds with sediment movement, standing waves, antidunes, chutes-and-pools). Although

83 Simons et al. (1961) noted that flows change from the lower to upper flow regimes at a Froude

84 number less than unity, Dey (2014) and Venditti (2013) stated that lower and upper flow regimes

85 are consistent with Froude-subcritical (Froude number < 1) and Froude-supercritical flow

86 regimes (Froude number > 1), respectively. In other words, two types of plane bed are

87 differentiated at Froude number = 1. On the other hand, Liu (1957) and Bogárdi (1961) reported

88 a region of flow conditions in which sediment motion occurred, but ripples or other bed relief did

89 not appear. Furthermore, the phase diagrams proposed by Allen (1968) and Southard (1971)

90 suggested that there is a stable plane bed region where coarse sediment (median diameter > 0.6-

91 0.7 mm) is transported at low flow velocities. This region is termed lower plane beds. Therefore,

92 Allen (1968) and Southard (1971) recognized two types of plane bed in addition to the plane bed

93 without sediment motion, which are lower plane beds on coarse-grained beds and plane beds in

94 the upper flow regime.

95   In this study, we propose new definitions of plane beds that explain existing experimental

96 and observational datasets well, compared to previous definitions. We compiled data pertaining

97 to plane beds in unidirectional open-channel flows, and plotted those using dimensionless

98 parameters as axes without any *a priori* assumption of types of plane bed. The compilation of a

99 large amount of existing data from the literature indicates that two classes of plane bed regimes

100 are recognized and the boundary between the two plane bed regimes matches the threshold

101 condition of suspension.

102

103 **2 Data Sources and Dimensionless Parameters for Morphodynamic Conditions**

104 We compiled a total of 937 sets of data pertaining to plane beds, from the literature, to

105 investigate the plane bed regimes. The dataset consisted of 892 sets of laboratory data and 45

106 sets of field data. Relevant references and the basic parameters are summarized in Table S1. A

107   wide range of hydraulic and sediment parameters are included in the datasets. The median

108   diameter D_{50} ranges from 11 μm to 44.3 mm, the flow depth h ranges from 1.2 mm to 2.74 m,

109   and the flow velocity U ranges 0.0448 to 2.38 m/s. Further, the data is classified into three types

110   based on the suspended sediment concentration C_s, as follows: (a) the suspended sediment

111   concentration was measured (hereafter referred to as data $C_s > 0$), (b) the suspended sediment

112   concentration was recorded as zero or the bed material did not move (hereafter referred to as data

113    $C_s = 0$), and (c) the suspended sediment concentration was not available (hereafter referred to as

114   data no C_s).

115   First, the hydraulic conditions of plane bed regimes were examined with the sediment

116   diameter and the sediment transport mechanism by which the sediment was moved, i.e., no

117   sediment movement, bed-load, and suspended load. Bedform phases were expressed in the space

118   of dimensionless parameters that reflected the properties of flows and sediment particles (Ohata

119   et al., 2017; van den Berg & van Gelder, 1993). In this study, we employed the following

120   dimensionless parameters to represent hydraulic conditions and sediment properties: the particle

121   Reynolds number $\mathrm{Re_p}$, Shields number τ_*, and the suspension index u_*/w_s.

122   The particle Reynolds number $\mathrm{Re_p}$ is defined as:

$$\mathrm{Re_p} = \frac{\sqrt{RgD_{50}}\,D_{50}}{\nu} \#(1)$$

123   where R represents the submerged specific gravity of the sediment, g denotes the gravitational

124   acceleration, and ν denotes the kinematic viscosity of the fluid. The submerged density is

125   defined as $R = (\rho_s - \rho_f)/\rho_f$, where ρ_s and ρ_f represents the sediment and fluid densities,

126   respectively. The kinematic viscosity ν was assumed to be a function of temperature according to

127   the relationship for clear, fresh water (van den Berg & van Gelder, 1993):

$$\nu = [1.14 - 0.031(T - 15) + 0.00068(T - 15)^2]10^{-6} \quad \#(2)$$

128   where T represents the water temperature in degrees Celsius. A value of 20 °C was assumed for

129   data where T was not reported. Shields number τ_* is defined as:

$$\tau_* = \frac{u_*^2}{RgD_{50}} \quad \#(3)$$

130   Here, the shear velocity u_* for the field data was computed as $u_* = \sqrt{ghS}$, where S represents

131   the slope. For laboratory data, the side-wall effect was removed using the method proposed by

132   Chiew & Parker (1994) (see Ohata et al. (2017) for details), and we calculated the bed

133   component of the shear velocity. The suspension index is expressed as the ratio of the shear

134   velocity u_* to the settling velocity of sediment w_s. The settling velocity w_s was estimated using

135   the relationship formulated by Ferguson & Church (2004):

$$w_s = \frac{RgD_{50}^2}{C_1\nu + \sqrt{0.75C_2RgD_{50}^3}} \quad \#(4)$$

136   where constants C_1 and C_2 were set to 18 and 1, respectively.

137   The sediment transport regimes are classified based on the transport mechanism—no

138   sediment movement, bed-load dominated, mixed-load, and suspended-load dominated regimes

139   (Church, 2006). The boundary between no sediment movement and other regimes is defined by

140   Shields curve, which is the critical condition for the initiation of particle motion (e.g., Shields,

141   1936). Based on Shields' experimental data, Brownlie (1981a) proposed a function describing

142   the threshold condition of particle motion as:

$$\tau_c^* = 0.22\mathrm{Re_p}^{-0.6} + 0.06\exp(-17.77\mathrm{Re_p}^{-0.6}) \quad \#(5)$$

143   Next, the critical condition for the initiation of suspension is expressed using the suspension

144   index u_*/w_s (Bagnold, 1966; van Rijn, 1984; NiÑo et al., 2003). The critical condition of

145   suspension represents the boundary between the bed-load dominated regime and a regime where

146   the bed materials are transported with suspension. The threshold condition for suspension,

147   obtained by NiÑo et al. (2003), is:

$$\frac{u_*}{w_s} = \begin{cases} 21.2\text{Re}_p^{-1.2}, & 1 < \text{Re}_p < 27.3 \\ 0.4, & 27.3 \leq \text{Re}_p \end{cases} \#(6)$$

148   Therefore, the region below equation (5) denotes the no sediment movement regime, the region

149   between equations (5) and (6) denotes a bed-load dominated regime, and the region above

150   equation (6) denotes mixed-load or suspended-load dominated regimes where the bed materials

151   are moved with suspension.

152   Second, the formation conditions of the plane bed regimes were investigated using

153   Froude number. The phase diagrams were obtained using Re_p, u_*/w_s, and Froude number as the

154   axes. Froude number is the ratio of the inertial force to the gravitational force, defined as:

$$\text{Fr} = \frac{U}{\sqrt{gh}} \#(7)$$

155   Here, the inertial force is represented by the flow velocity U and the gravitational force $\sqrt{gh}$

156   denotes the velocities of the free-surface waves. Flows with Fr < 1 and Fr > 1 are called Froude-

157   subcritical and Froude-supercritical flows, respectively.

158 **3 Results**

159 3.1 Sediment transport mode and plane bed formation

160 First, the plane bed data were plotted in $\mathrm{Re_p} - \tau_*$ space (Figure 1a) to investigate the relationships

161 among the plane bed regimes, the particle diameter, and the criteria for sediment movement. The

162 threshold condition of particle motion (equation (5)) and suspension (equation (6)) are described

163 in Figure 1a. Threshold condition of suspension (equation (6)) was rearranged using equations

164 (1), (3), and (4) where $R = 1.65$ and $v = 1.0 \times 10^{-6}$. The median diameter D_{50} is also recasted

165 from $\mathrm{Re_p}$ with $R = 1.65$ and $v = 1.0 \times 10^{-6}$, which is represented on the top axis of Figure 1a.

166   Shields number of the plane bed ranges from 0.05 to 10, and the plane bed data are

167 divided into two separate regions at $\tau_* = 0.1–0.2$ (Figure 1a). The plane bed data with low τ_* plot

168 around the threshold condition of particle motion, and the region with high τ_* plots above the

169 threshold condition of suspension. The threshold condition of particle motion does not divide the

170 plane bed regime; rather, the threshold condition of suspension runs between the two regions of

171 data. The particle Reynolds number of the data with low and high τ_* ranges as follows: $9 < \mathrm{Re_p}$

172 $< 4.0 \times 10^4$ (0.2 mm $< D_{50} <$ 40 mm) and $0.1 < \mathrm{Re_p} < 300$ (0.01 mm $< D_{50} <$ 2 mm),

173 respectively. The data $C_s > 0$ and field observation data are included in the region of high τ_*.

174 Most data $C_s = 0$ plot around the criteria for particle motion, and three points of data $C_s = 0$ plot
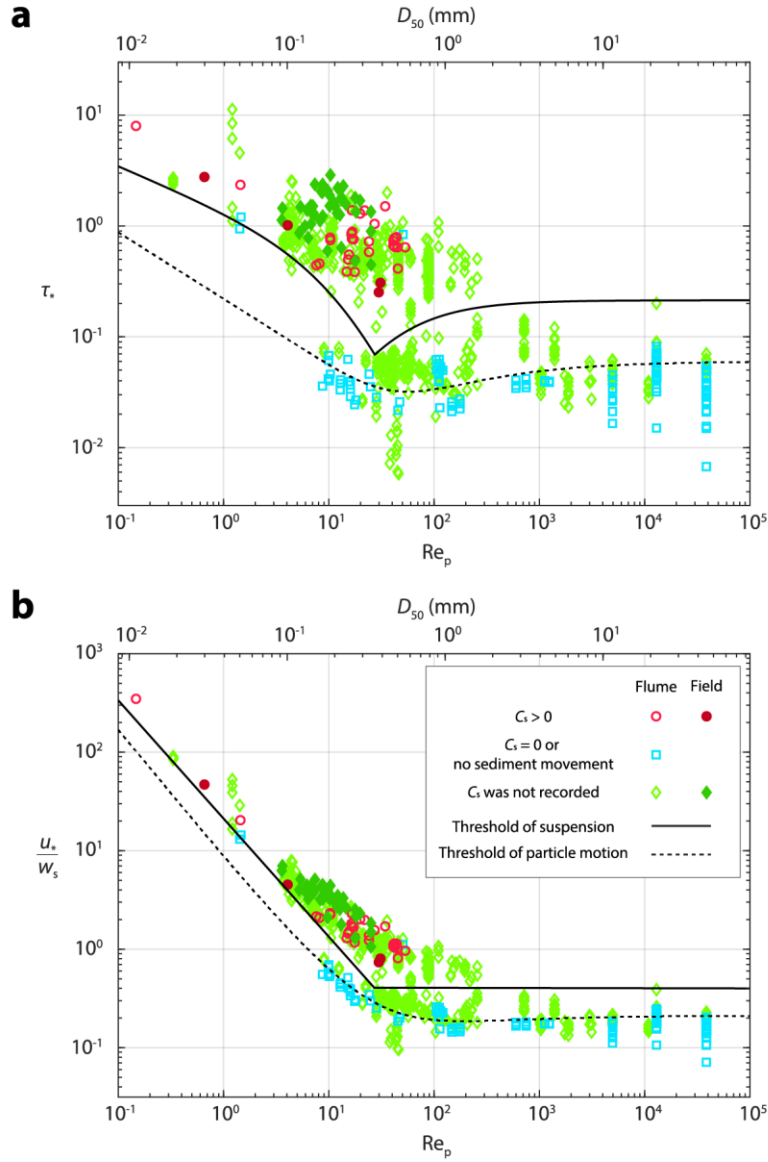
175 around $\tau_* = 1$.

176

Figure 1. Plane bed regime in (a) $\mathrm{Re_p}-\tau_*$ space and (b) $\mathrm{Re_p}-u_*/w_s$ space. The dotted line

denotes the threshold condition for particle motion (equation (5)). The solid line denotes the

threshold condition for suspension (equation (6)). Both lines were extended to $\mathrm{Re_p} = 10^{-1}$ and

10^5.

181

182 Second, the relationships among the plane bed regimes, the sediment diameter, and the

183 criteria for suspension were examined by plotting u_*/w_s versus Re_p (Figure 1b). The threshold

184 condition of suspension (equation (6)), and for comparison, the threshold condition of particle

185 motion (equation (5)) are described in Figure 1b. To plot equation (5) in Re_p–u_*/w_s space, R

186 and v were assigned the values 1.65 and 1.0×10^{-6}, respectively. The median diameter D_{50} is

187 depicted on the top side of Figure 1b.

188 Figure 1b shows that the plane bed data plot in two regions separated by the threshold

189 condition of suspension as well as in Re_p–τ_* space (Figure 1a). The threshold condition of

190 particle motion runs through the middle of the data with a low suspension index. With respect to

191 the particle Reynolds number, the data with high suspension index plot in the region $0.1 < \text{Re}_p <$

192 3200 (0.01 mm $< D_{50} < 2$ mm) and the data with low suspension index plot in the region $9 < \text{Re}_p$

193 $< 4.0 \times 10^4$ (0.2 mm $< D_{50} < 40$ mm). The data $C_s > 0$ and field observation data plot above the

194 threshold condition of suspension. Most data $C_s = 0$ plot along the criteria for particle motion,

195 although a few points of data $C_s = 0$ plot above the suspension criteria.

196

197 3.2 Impact of Froude number

198 The consistency of the flow regime concept based on Froude number (Dey, 2014;

199 Venditti 2013) to plane bed regimes was investigated using the diagrams described in Re_p–Fr

200 (Figure 2a) and u_*/w_s–Fr spaces (Figure 2b).

201 Figure 2 shows that all the data covers a wide range of Froude number ranging from 0.1

202 to 3.5, and the separated regions cannot be seen on the Froude number axis. The field

203 observations data have a lower Froude number (Fr < 0.5), whereas the field data exceed 0.7 in

204   the suspension index and plot above the threshold condition of suspension (Figure 1b). For $C_s >$

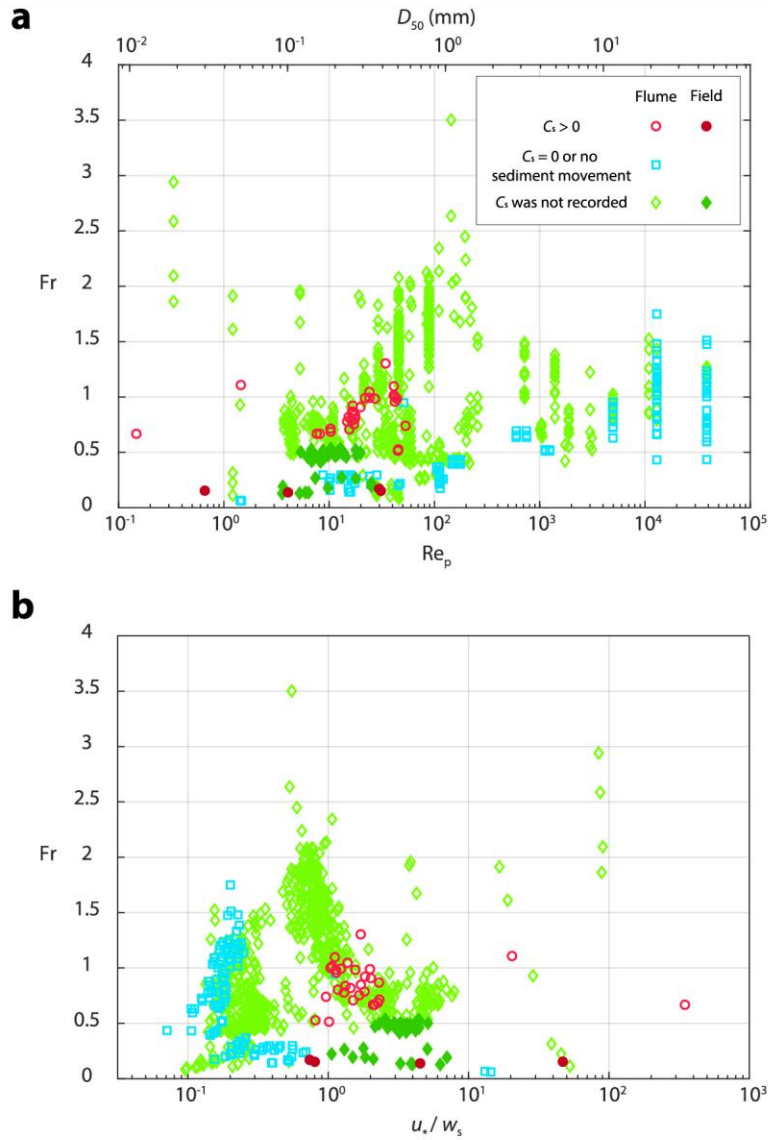205   0, the data fall in the domain $0.1 < Fr < 1.3$, and the data $C_s = 0$ distribute in the domain $0.2 < Fr$

206   < 1.0.

207

208

209   **Figure 2.** Plane bed regime in (a) Re_p–Fr space and (b) u_*/w_s–Fr space.

210   **4 Discussion**

211   Data from the existing field observations and flume experiments for plane beds were collected to

212   revisit the formation conditions of plane beds. The phase diagrams indicate that the phase

213   regions of the plane beds are not separated by particle diameter or the criticalities of sediment

214   motion and Froude number, which were used to classify the lower and upper plane beds. In

215   contrast, observational data of the plane beds plot in two separate regions in the $\mathrm{Re_p}{-}\tau_*$ and

216    $\mathrm{Re_p}{-}u_*/w_\mathrm{s}$ diagrams, and the boundary between the two regions matches the threshold

217   condition for suspension. Therefore, our phase diagrams suggest that the upper and lower plane

218   bed phases are redefined—the upper plane beds are plane beds with suspension, and the lower

219   plane beds are plane beds without suspension.

220   The new definition of upper plane beds is consistent with previous studies that describe

221   the phase diagrams of bedforms based on theoretical analysis (Nakasato & Izumi, 2008).

222   Nakasato & Izumi (2008) performed linear stability analysis considering active suspended loads

223   and demonstrated that dune formation is suppressed by suspended loads. Further, the

224   contribution of suspension to the formation of plane beds from dunes has been observed in flume

225   and numerical experiments (Naqshband et al., 2015; Naqshband et al., 2017; Bradley & Venditti,

226   2019). The bed-load transport plays a vital role in the formation of stable dunes (Naqshband et

227   al., 2014; Bradley & Venditti, 2019), whereas dune height decreases as more bed particles are

228   transported as suspended loads (Naqshband et al., 2017; Bradley & Venditti, 2019).

229   According to Figure 1a, our compiled datasets indicate that the previous definitions of

230   lower plane beds by Simons et al. (1961) and Southard (1971) do not demonstrate the two

231   separated regimes of plane beds. In previous studies, lower plane beds were defined as plane

232   beds without sediment motion (Simons et al., 1961) or plane beds just above the threshold of

233   sediment motion under subcritical flow with coarse grains (Southard, 1971). In Figure 1a, two

234   separated regimes that have low Shields number ($\tau_* < 0.1$–0.2) and high Shields number ($\tau_* >$

235   0.1–0.2) are observed. For the data with low Shields number ($\tau_* < 0.1$–0.2), plane beds can

236   appear with finer sediments ($D_{50} < 0.6$–0.7 mm) and the threshold condition of particle motion

237   plot through the middle of the data scatter. This suggests that the traditional definitions of plane

238   beds by Simons et al. (1961) and Southard (1971) are inconsistent with the dataset.

239   It is noteworthy that Froude number has a small impact on the formation of the plane

240   beds, and there are no gaps in Froude number as shown in Figure 2. Froude number for the field

241   data can be lower than unity, due to the great depth of natural rivers, and when the shear stress

242   for the field data is high. Indeed, Ma et al. (2017) conducted field surveys at the Yellow River,

243   China, measureing sediment loads and bed topography, and observed a nearly flat bed with low

244   Froude number (Fr = 0.23). The ratio of length to height of the bed waves ranged from 500 to

245   2000, which is a much higher ratio than that of dunes in other natural rivers (Ma et al., 2017).

246   They estimated the hydraulic resistance in the Yellow River based on Engelund–Hansen

247   sediment transport theory (Engelund & Hansen, 1967) and found that the bed resistance was

248   similar to that of plane bed. Shields number in the Yellow River was 1.05 with $D_{50} = 0.09$ mm,

249   which would plot above the threshold condition of suspension (see Figure 1a), implying that the

250   bedform observed in the Yellow River corresponds to the upper plane bed defined in this study.

251   To summarize, the lower and upper plane beds cannot be defined by Froude number, as stated by

252   Dey (2014) and Venditti (2013).

253   Similarly, our phase diagrams imply that the origin of parallel laminae in sandstones

254   cannot be presumed as the upper plane bed. Previous studies suggest that the lower and upper

255   plane beds can be distinguished by grain size, therefore, fine-grained parallel lamination has

256 been considered as the upper plane bed deposits. Best & Bridge (1992), whose experimental

257 results were compared with parallel laminated sandstones, assumed that the laminae were

258 produced by the upper plane bed. However, lower plane beds can also form with fine-grained

259 materials, as depicted in Figure 1. Subsequently, it is difficult to distinguish from the outcrops

260 whether the parallel laminae were formed with or without suspension. This study suggests that

261 much remains to be done theoretically and experimentally to interpret the flow conditions that

262 form parallel lamination. To this end, detailed characterizations of parallel laminae from lower

263 and upper plane beds are required under controlled conditions in flume experiments.

264 The origin of the lower plane bed phase in the new definition is puzzling. In previous

265 studies, the controlling factor in the lower and upper plane bed regimes was assumed to be the

266 grain size. Leeder (1980) interpreted that coarse-grained plane beds are formed because flow

267 separation is prevented by the bed roughness. Recently, Blois et al. (2014) proposed that bed

268 permeability may be another explanation for the formation of coarse-grained plane beds.

269 However, this study established that the region of coarse-grained plane beds extends

270 continuously to the fine-grained region, and the conditions for fine-grained plane beds were

271 distributed separately in the two regions: the high- and low-bed shear stress. Thus, the formation

272 of the lower plane bed cannot be attributed to bed roughness or permeability owing to the grain

273 size distribution.

274 It should be noted here that bed particles are also transported by sheet flows (Sumer et al.,

275 1996), which may potentially be related to the plane bed. The sheet flow consists of a shear layer

276 of bed load and occurs at high shear stress where ripples and dunes are washed out (Pugh &

277 Wilson, 1999; Sumer et al., 1996). The laboratory experiments for sheet flows have been

278 conducted using a closed conduit in order to achieve high shear stresses and avoid the free-

279   surface effect (Nnadi & Wilson, 1992; Sumer et al., 1996) or under oscillatory flows to simulate

280   storm conditions that change the beach surface (Dick & Sleath, 1992; O'Donoghue & Wright,

281   2004). The sheet flow regime is not described in our phase diagram because this study focuses

282   on the unidirectional open-channel flows. Experiments for sheet flows in open-channel flows are

283   scarce. Therefore, currently, it is difficult to determine whether the sheet flow is another possible

284   mechanism that generates plane beds. Thus, further laboratory experiments, numerical

285   experiments, and theoretical consideration are required to provide explanations for the lower

286   plane bed regime.

287

288

289   **5 Conclusions**

290   In the present study, we compiled 937 flume and field data sets pertaining to plane beds and

291   analyzed the dataset in the nondimensional parametric space. The results of our analysis indicate

292   that the formation conditions of plane beds are distributed in two separate regions, and the

293   boundary between the regions matches the threshold condition for suspension. Therefore, the

294   upper and lower plane beds can be redefined as plane beds with and without suspension,

295   respectively. Conversely, the formation conditions of plane beds do not show a clear boundary at

296   the threshold condition of sediment motion, a unique value of particle diameter, or a Froude

297   number of unity, which have been traditionally used to define lower and upper plane beds. This

298   study demonstrates that the existence of suspension significantly contributes to the formation of

299   plane beds, whereas other mechanisms can also produce fine-grained plane beds in flows with

300   low-bed shear stress.

301

308

References

310

311 Allen, J. R. L. (1968). *Current ripples: Their relation to patterns of water and sediment motion*.

312 Amsterdam, Netherlands: North Holland Publishing Company.

313 Baird, D. C. (2010). Field adjustments of bed form phase diagrams. 2nd Joint Federal

314 Interagency Conference. Las Vegas, NV.

315 Bagnold, R. A. (1966). *An approach to the sediment transport problem from general physics*

316 (Geological Survey Professional Paper 422-I). Washington, DC: United States

317 Government Printing Office.

318 Barton, J. R., & Lin, P. N. (1955). *A study of the sediment transport in alluvial channels* (Report

319 No. CEF 55JRB2). Fort Collins, CO: Colorado State University.

320   Best, J. (2005). The fluid dynamics of river dunes: A review and some future research directions.

321   *Journal of Geophysical Research: Earth Surface*, *110*(4), F04S02.

322   https://doi.org/10.1029/2004JF000218

323   Best, J., & Bridge, J. (1992). The morphology and dynamics of low amplitude bedwaves upon

324   upper stage plane beds and the preservation of planar laminae. *Sedimentology*, *39*(5),

325   737–752. https://doi.org/10.1111/j.1365-3091.1992.tb02150.x

326   Blois, G., Best, J. L., Sambrook Smith, G. H., & Hardy, R. J. (2014). Effect of bed permeability

327   and hyporheic flow on turbulent flow over bed forms. *Geophysical Research Letters*,

328   *41*(18), 6435–6442. https://doi.org/10.1002/2014GL060906

329   Bogárdi, J. (1961). Some aspects of the application of the theory of sediment transportation to

330   engineering problems. *Journal of Geophysical Research*, *66*(10), 3337–3346.

331   https://doi.org/10.1029/JZ066i010p03337

332   Bouma, A. H. (1962). *Sedimentology of some flysch deposits: A graphic approach to facies*

333   *interpretation*. Amsterdam, Netherlands: Elsevier Scientific Publishing Company.

334   Bradley, R. W., & Venditti, J. G. (2019). Transport scaling of dune dimensions in shallow flows.

335   *Journal of Geophysical Research: Earth Surface*, *124*(2), 526–547.

336   https://doi.org/10.1029/2018JF004832

337   Bridge, J. S., & Best, J. L. (1988). Flow, sediment transport and bedform dynamics over the

338   transition from dunes to upper-stage plane beds: Implications for the formation of planar

339   laminae. *Sedimentology*, *35*(5), 753‑763. https://doi.org/10.1111/j.1365-

340   3091.1988.tb01249.x

341 Brooks, N. H. (1955). Mechanics of streams with movable beds of fine sand. *Proceedings of the*

342   *American Society of Civil Engineers*, *81*(668), 1–28.

343 Brownlie, W. R. (1981a). *Prediction of flow depth and sediment discharge in open channels*

344   (Report No. KH-R-43A). Pasadena, CA: W. M. Keck Laboratory of Hydraulics and

345   Water Resources, California Institute of Technology.

346 Brownlie, W. R. (1981b). *Compilation of fluvial channel data: Laboratory and field* (Report No.

347   KH-R-43B). Pasadena, CA: W. M. Keck Laboratory of Hydraulics and Water Resources,

348   California Institute of Technology.

349 Cao, H. H. (1985). *Résistance hydraulique d'un lit de gravier mobile à pente raide: étude*

350   *expérimentale* (Ph.D. Thesis). Lausanne, Switzerland: Ecole Polytechnique Fédérale de

351   Lausanne.

352 Chiew, Y.-M., & Parker, G. (1994). Incipient sediment motion on non-horizontal slopes. *Journal*

353   *of Hydraulic Research*, *32*(5), 649–660. https://doi.org/10.1080/00221689409498706

354 Church, M. (2006). Bed material transport and the morphology of alluvial river channels. *Annual*

355   *Review of Earth and Planetary Sciences*, *34*(1), 325–354.

356   https://doi.org/10.1146/annurev.earth.33.092203.122721

357 Chyn, S. D. (1935). *An experimental study of the sand transporting capacity of the flowing water*

358   *on sandy bed and the effect of the composition of the sand* (master's thesis). Cambridge,

359   MA: Massachusetts Institute of Technology.

360 Colby, B. R., & Hembree, C. H. (1955). *Computations of total sediment discharge, Niobrara*

361   *River near Cody, Nebraska* (Geological Survey Water-Supply Paper 1357). Washington,

362   DC: United States Government Printing Office.

363   Colombini, M., & Stocchino, A. (2008). Finite-amplitude river dunes. *Journal of Fluid*

364   *Mechanics*, *611*, 283–306. https://doi.org/10.1017/S0022112008002814

365   Costello, W. R. (1974). *Development of bed configuration in coarse sands* (Report No. 74-1).

366   Cambridge, MA: Massachusetts Institute of Technology.

367   Culbertson, J. K., Scott, C. H., & Bennet, J. P. (1972). *Summary of alluvial-channel data from*

368   *Rio Grande conveyance channel, New Mexico, 1965–69* (Geological Survey Professional

369   Paper 562-J). Washington, DC: United States Government Printing Office.

370   Dey, S. (2014). *Fluvial hydrodynamics: Hydrodynamic and sediment transport phenomena.*

371   Berlin, Germany: Springer.

372   Dick, J. E., & Sleath, J. F. A. (1992). Sediment transport in oscillatory sheet flow. *Journal of*

373   *Geophysical Research*, *97*(C4), 5745–5758. https://doi.org/10.1029/92JC00054

374   East Pakistan Water and Power Development Authority (1966,1968-1969), *Flume studies of*

375   *roughness and sediment transport of movable bed of sand*, Annual Report of Hydraulic

376   Research Laboratory, Dacca.

377   Eggenhuisen, J. T., McCaffrey, W. D., Haughton, P. D. W., & Butler, R. W. H. (2011). Shallow

378   erosion beneath turbidity currents and its impact on the architectural development of

379   turbidite sheet systems. *Sedimentology*, *58*(4), 936–959. https://doi.org/10.1111/j.1365-

380   3091.2010.01190.x

381   Engelund, F., & Hansen, E. (1967). A monograph on sediment transport in alluvial streams.

382   Copenhagen, Denmark: Teknisk Forlag.

383   Ferguson, R. I., & Church, M. (2004). A simple universal equation for grain settling velocity.

384   *Journal of Sedimentary Research*, *74*(6), 933–937. https://doi.org/10.1306/051204740933

385 Fukuoka, S., Okutsu, K., & Yamasaka, M. (1982). Dynamic and kinematic features of sand

386   waves in upper regime (in Japanese). *Proceedings of the Japan Society of Civil Engineers*,

387   *323*, 77–89. https://doi.org/10.2208/jscej1969.1982.323_77

388 Gee, D. M. (1975). Bed form response to nonsteady flows. *Journal of the Hydraulics Division*,

389   *101*(HY3), 437–449.

390 Gilbert, G. K. (1914). *The transportation of debris by running water* (Geological Survey

391   Professional Paper 86). Washington, DC: United States Government Printing Office.

392 Guy, H. P., Simons, D. B., & Richardson, E. V. (1966). *Summary of alluvial channel data from

393   flume experiments, 1956–61* (Geological Survey Professional Paper 462-I). Washington,

394   DC: United States Government Printing Office.

395 Hauer, C., Holzapfel, P., Tonolla, D., Habersack, H., & Zolezzi, G. (2019). In situ measurements

396   of fine sediment infiltration (FSI) in gravel-bed rivers with a hydropeaking flow regime.

397   *Earth Surface Processes and Landforms*, *44*(2), 433–448.

398   https://doi.org/10.1002/esp.4505

399 Jobe, Z. R., Lowe, D. R., & Morris, W. R. (2012). Climbing-ripple successions in turbidite

400   systems: Depositional environments, sedimentation rates and accumulation times.

401   *Sedimentology*, *59*(3), 867–898. https://doi.org/10.1111/j.1365-3091.2011.01283.x

402 Jopling, A. V, & Forbes, D. L. (1979). Flume study of silt transportation and deposition.

403   *Geografiska Annaler. Series A, Physical Geography*, *61*, 67–85.

404   https://doi.org/10.1080/04353676.1979.11879983

405 Jorissen, A. L. (1938). Étude expérimentale du transport solide des cours d'eau. *Revue

406   Universelle Des Mines*, *14*(3), 269–282.

407   Julien, P. Y., & Raslan, Y. (1998). Upper-regime plane bed. *Journal of Hydraulic Engineering*,

408   *124*(11), 1086–1096. https://doi.org/10.1061/(ASCE)0733-9429(1998)124:11(1086)

409   Kalinske, A. A., & Hsia, C. H. (1945). *Study of transportation of fine sediments by flowing water*

410   (Bulletin No. 29), University of Iowa Studies in Engineering.

411   Kennedy, J. F. (1961). Stationary waves and antidunes in alluvial channels (Report No. KH-R-2).

412   Pasadena, CA: W. M. Keck Laboratory of Hydraulics and Water Resources, California

413   Institute of Technology. https://doi.org/10.7907/Z9QR4V22

414   Kennedy, J. F., & Brooks, N. H. (1963). Laboratory study of an alluvial stream of constant

415   discharge. in *Proceedings of the Federal Inter-Agency Sedimentation Conference*, 320–

416   330.

417   Kuhnle, R. A., & Wren, D. G. (2009). Size of suspended sediment over dunes. *Journal of*

418   *Geophysical Research: Earth Surface*, *114*(2), 1–9.

419   https://doi.org/10.1029/2008JF001200

420   Laursen, E. M. (1958). The total sediment load of streams. *Journal of the Hydraulics Division*,

421   *84*(1), 1–36.

422   Leeder, M. R. (1980). On the stability of lower stage plane beds and the absence of current

423   ripples in coarse sands. *Journal of the Geological Society*, *137*(4), 423–429.

424   https://doi.org/10.1144/gsjgs.137.4.0423

425   Liu, H.-K. (1957). Mechanics of sediment-ripple formation. *Journal of the Hydraulics Division*,

426   *83*(2), 1–23.

427   Ma, H., Nittrouer, J. A., Naito, K., Fu, X., Zhang, Y., Moodie, A. J., … Parker, G. (2017). The

428   exceptional sediment load of fine-grained dispersal systems: Example of the Yellow

429   River, China. *Science Advances*, *3*(5). https://doi.org/10.1126/sciadv.1603114

430   Mahmood, K., Tarar, R. N., Hassan, S. A., Khan, H., & Masood, T. (1979). *Selected*

431   *equilibrium-state data from ACOP Canals* (Rep. No. EWR-79-2). Washington, DC: Civil

432   Mechanical and Environmental Engineering Department, George Washington University.

433   Mazumder, R., & Van Kranendonk, M. J. (2013). Palaeoproterozoic terrestrial sedimentation in

434   the Beasley River Quartzite, lower Wyloo Group, Western Australia. *Precambrian*

435   *Research*, *231*, 98–105. https://doi.org/10.1016/J.PRECAMRES.2013.03.018

436   Mutter, D. G. (1971). *A flume study of alluvial bed configurations* (master's thesis). Alberta,

437   Canada: Faculty of Graduate Studies, University of Alberta.

438   Nakasato, Y., & Izumi, N. (2008). Linear stability analysis of small-scale fluvial bed waves with

439   active suspended sediment load (in Japanese with English abstract). *Journal of Applied*

440   *Mechanics*, *11*, 727–734. https://doi.org/10.2208/journalam.11.727

441   Naqshband, S., van Duin, O., Ribberink, J., & Hulscher, S. (2015). Modeling river dune

442   development and dune transition to upper stage plane bed. *Earth Surface Processes and*

443   *Landforms*, *41*(3), 323–335. https://doi.org/10.1002/esp.3789

444   Naqshband, S., Hoitink, A. J. F., McElroy, B., Hurther, D., & Hulscher, S. J. M. H. (2017). A

445   sharp view on river dune transition to upper stage plane bed. *Geophysical Research*

446   *Letters*, *44*(22), 11,437–11,444. https://doi.org/10.1002/2017GL075906

447   Naqshband, S., Ribberink, J. S., Hurther, D., & Hulscher, S. J. M. H. (2014). Bed load and

448   suspended load contributions to migrating sand dunes in equilibrium. *Journal of*

449   *Geophysical Research: Earth Surface*, *119*(5), 1043–1063.

450   https://doi.org/10.1002/2013JF003043

451 Neill, C. R. (1969). Bed forms in the lower Red Deer River, Alberta. *Journal of Hydrology*, *7*,

452   58–85.

453 NiÑo, Y., Lopez, F., & Garcia, M. (2003). Threshold for particle entrainment into suspension.

454   *Sedimentology*, *50*(2), 247–263. https://doi.org/10.1046/j.1365-3091.2003.00551.x

455 Nnadi, F. N., & Wilson, K. C. (1992). Motion of contact-load particles at high shear stress.

456   *Journal of Hydraulic Engineering*, *118*(12), 1670–1684.

457   https://doi.org/10.1061/(ASCE)0733-9429(1992)118:12(1670)

458 Nomicos, G. N. (1956). *Effects of sediment load on the velocity field and friction factor of*

459   *turbulent flow in an open channel* (Ph.D. thesis). Pasadena, CA: California Institute of

460   Technology.

461 Nordin, C. F. (1976). *Flume studies with fine and coarse sands* (Open File Report No. 76-762).

462   Washington, DC: US Geological Survey.

463 O'Donoghue, T., & Wright, S. (2004). Concentrations in oscillatory sheet flow for well sorted

464   and graded sands. *Coastal Engineering*, *50*(3), 117–138.

465   https://doi.org/10.1016/j.coastaleng.2003.09.004

466 Ohata, K., Naruse, H., Yokokawa, M., & Viparelli, E. (2017). New bedform phase diagrams and

467   discriminant functions for formative conditions of bedforms in open-channel flows.

468   *Journal of Geophysical Research: Earth Surface*, *122*(11), 2139–2158.

469   https://doi.org/10.1002/2017JF004290

470   Owens, J. S. (1908). Experiments on the transporting power of sea currents. *The Geographical*

471   *Journal*, *31*(4), 415–420. https://doi.org/10.2307/1777846

472   Pratt, C. J. (1970). *Summary of experimental data for flume tests over 0.49 mm sand*.

473   Southampton, England: Department of Civil Engineering, University of Southampton.

474   Pugh, F. J., & Wilson, K. C. (1999). Velocity and concentration distributions in sheet flow above

475   plane beds. *Journal of Hydraulic Engineering*, *125*(2), 117–125.

476   https://doi.org/10.1061/(ASCE)0733-9429(1999)125:2(117)

477   Rathbun, R. E., & Guy, H. P. (1967). Measurement of hydraulic and sediment transport variables

478   in a small recirculating flume. *Water Resources Research*, *3*(1), 107–122.

479   https://doi.org/10.1029/WR003i001p00107

480   Shields, A. (1936). *Application of similarity principles and turbulence research to bed-load*

481   *movement* (English translation of an original German manuscript). Pasadena, CA: Soil

482   Conservation Service Cooperative Laboratory, California Institute of Technology.

483   Simons, D. B. (1957). *Theory and design of stable channels in alluvial material* (Ph.D. thesis).

484   Fort Collins, CO: Colorado State University.

485   Simons, D. B., Richardson, E. V., & Albertson, M. L. (1961). *Flume studies using medium sand*

486   *(0.45 mm)* (Geological Survey Water-Supply Paper 1498-A). Washington, DC: United

487   States Government Printing Office.

488   Simons, D. B., & Richardson, E. V. (1962). *The effect of bed roughness on depth-discharge*

489   *relations in alluvial channels* (Geological Survey Professional Paper 1498-E).

490   Washington, DC: United States Government Printing Office.

491   Singh, B. (1960). *Transport of bed-load in channels with special reference to gradient and form*

492   (Ph.D. thesis). London, England: University of London.

493   Southard, J. B. (1971). Representation of bed configurations in depth-velocity-size diagrams.

494   *Journal of Sedimentary Research*, *41*(4), 903–915. https://doi.org/10.1306/74D723B0-

495   2B21-11D7-8648000102C1865D

496   Stein, R. A. (1965). Laboratory studies of total load and apparent bed load. *Journal of*

497   *Geophysical Research*, *70*(8), 1831–1842. https://doi.org/10.1029/JZ070i008p01831

498   Strahan, A., Lamplugh, M., Cornish, V., Mill, D., Evans, D., Tizard, C., … Owens, J. S. (1908).

499   Experiments on the transporting power of sea currents: Discussion. *The Geographical*

500   *Journal*, *31*(4), 420–425. https://doi.org/10.2307/1777847

501   Sumer, B. M., Kozakiewicz, A., Fredsøe, J., & Deigaard, R. (1996). Velocity and concentration

502   profiles in sheet-flow layer of movable bed. *Journal of Hydraulic Engineering*, *122*(10),

503   549–558. https://doi.org/10.1061/(ASCE)0733-9429(1996)122:10(549)

504   Taki, K., & Parker, G. (2005). Transportational cyclic steps created by flow over an erodible bed.

505   Part 1. Experiments. *Journal of Hydraulic Research*, *43*(5), 488–501.

506   https://doi.org/10.1080/00221680509500147

507   Tanaka, Y. (1970). An experimental study on anti-dunes. *Disaster Prevention Research Institute*

508   *Annuals*, *13*(B), 271–284.

509   Taylor, B. D. (1971). *Temperature effects in alluvial streams* (Report No. KH-R-27). Pasadena,

510   CA: W. M. Keck Laboratory of Hydraulics and Water Resources, California Institute of

511   Technology.

512   Ueno, T. (1981). On the regions of occurrence of ripples and dunes (in Japanese). *Proceedings of*

513   *the Japanese Conference on Hydraulics*, *25*, 93–98.

514   https://doi.org/10.2208/prohe1975.25.93

515   Umazano, A. M., Bellosi, E. S., Visconti, G., & Melchor, R. N. (2012). Detecting allocyclic

516   signals in volcaniclastic fluvial successions: Facies, architecture and stacking pattern

517   from the Cretaceous of central Patagonia, Argentina. *Journal of South American Earth*

518   *Sciences*, *40*, 94–115. https://doi.org/10.1016/J.JSAMES.2012.09.005

519   United States Army Corps of Engineers, U.S. Waterways Experiment Station, Vicksburg,

520   Mississippi (1935). *Studies of river bed materials and their movement with special*

521   *reference to the lower mississippi river*, pp. 161. Vicksburg, MS: USWES.

522   van den Berg, J. H., & van Gelder, A. (1993). A new bedform stability diagram, with emphasis

523   on the transition of ripples to plane bed in flows over fine sand and silt. *Special*

524   *Publication of the International Association of Sedimentologists*, *17*, 11–21.

525   https://doi.org/10.1002/9781444303995.ch2

526   van Rijn, L. C. (1984). Sediment transport, Part II: Suspended load transport. *Journal of*

527   *Hydraulic Engineering*, *110*(11), 1613–1641.

528   Vanoni, V. A., & Brooks, H. (1957). *Laboratory studies of the roughness and suspended load of*

529   *alluvial streams* (Report No. E-68). Pasadena, CA: W. M. Keck Laboratory of Hydraulics

530   and Water Resources, California Institute of Technology.

531   Vaucher, R., Pittet, B., Passot, S., Grandjean, P., Humbert, T., & Allemand, P. (2018). Bedforms

532   in a tidally modulated ridge and runnel shoreface (Berck-Plage; North France):

533   implications for the geological record. *Bulletin de La Société Géologique de France*,

534   *189*(1), 5. https://doi.org/10.1051/bsgf/2018004

535   Venditti, J. G. (2013). Bedforms in sand-bedded rivers. In J. Shroder & E. Wohl (Eds.), *Treatise*

536   *on geomorphology* (Vol. 9, pp. 137–162). San Diego, CA: Academic Press.

537   https://doi.org/10.1016/B978-0-12-374739-6.00235-9

538   Williams, G. P. (1970). *Flume width and water depth effects in sediment transport experiments*

539   (Geological Survey Professional Paper 562-H). Washington, DC: United States

540   Government Printing Office.

541   Willis, J. C., Coleman, N. L., & Ellis, W. M. (1972). Laboratory study of transport of fine sand.

542   *Journal of the Hydraulics Division*, *98*(3), 489–501.

543   Yokokawa, M., Takahashi, Y., Yamamura, H., Kishima, Y., Parker, G., & Izumi, N. (2011).

544   Phase diagram for antidunes and cyclic steps based on suspension index, non-

545   dimensional Chezy resistance coefficient and Froude number. *Proceedings of the*

546   *International Association for Hydro-Environment Engineering and Research, 7th*

547   *Symposium on River, Coastal and Estuarine Morphodynamics (RCEM 2011)*, 1789–1794.

548   Znamenskaya, N. S. (1963). *Experimental study of the dune movement of sediment*. Soviet

549   Hydrology, Selected Papers. pp. 253–275. Washington, DC: American Geophysical

550   Union.

551